Dissolution rates of chemical components of an Insensitive High Explosive formulation

Encina Gutierrez-Carazo *[a], Frederic Coulon [b], Tracey Temple [a], Melissa Ladyman [a]

[a] Cranfield University, Centre for Defence Chemistry, Defence Academy of the United Kingdom, Shrivenham SN6 7LA, UK

[b] Cranfield University, School of Water, Energy and Environment, Cranfield, MK43 0AL, UK

ABSTRACT

The need for insensitive munitions has driven the replacement of traditional explosives by Insensitive High Explosives (IHE), which are less likely to detonate when accidentally hit. This new generation of formulations contains mixtures of compounds such as 2,4-dinitroanisole (DNAN) and 5-nitro-1,2,4-triazol-3-one (NTO) that have different physico-chemical properties potentially making them more labile and mobile through the environment. However, little is known about the persistence and toxicity of these chemicals once released in the environment, which raises the challenge of how they could be assessed for human exposure. Therefore, the aim of this study was to develop a computational model simulating the dissolution of the explosive formulation, i.e. simulating the rate at which residues may enter into the environment after deposition of solid particles. Dissolution tests were conducted on three small flakes of the formulation to determine individual dissolution rates. These rates were then used as stochastic inputs to the model created in GoldSim. Computational results revealed variability between maximum and minimum dissolved mass over time for DNAN and RDX but especially for NTO. The simulation was used to estimate the persistence of the explosive chemicals in the environment using real rainfall data of Wiltshire, UK suggesting that in average, the flakes need over a year to completely dissolve. The final purpose of the model is to support environmental management strategies and evaluate impact caused by IHE formulations in the environment.

1. Introduction

Currently, explosive compounds are used extensively for military training (defence) and mining and demolition (industry) [1,2]. Activities such as explosive manufacturing, disposal and blow-in-place detonations are some of the main uses of these chemical compounds. However, there is growing public concern around their use as they remain in the environment after their release, leading to potential soil and water contamination. Explosives and their residues have been categorised as hazardous waste by the European Union and must be managed and disposed safely [3]. This type of contamination can cause increased toxicity exposure to flora [4] and fauna [5,6], as well as human health issues [7]. Therefore, it is necessary to assess explosive environmental impact in order to preserve ecosystems.

The need for safer munitions has driven the replacement of traditional explosive fills such as 2,4,6-trinitrotoluene (TNT), hexahydro-1,3,5-trinitro-1,3,5-triazine (RDX) and octahydro-1,3,5,7-tetranitro-1,3,5,7-tetrazocine (HMX) with IHE. This new generation contains chemical compounds such as DNAN and NTO, which are less likely to be detonated as a result of an accident. 2,4-dinitroanisole is frequently used as a binder for other explosive constituents such as 5-nitro-1,2,4-triazol-3-one and RDX (**Table 1**). NTO is highly soluble in water and an acidic compound (pKa 3.76), which quickly dissolves during periods of rainfall and therefore may easily travel through saturated and unsaturated environmental zones. In soils with high organic content, NTO rapidly degrades into 5-amino-1,2,4-triazol-3-one (ATO), and ultimately into nitrates. Although DNAN does not have explosive activity, it has been reported to remain immobilized in soils with high organic matter content and to undergo degradation into more toxic compounds such as 2-amino-4-nitroanisole (2-ANAN) and 2,4-diaminoanisole (DAAN) and dinitrophenol (DNP) [8]. Finally, RDX has low solubility in water and tends not to degrade in the environment. It has been reported to be toxic for animals and can accumulate in leaves of plants [9]. The effects of RDX in the environment have been widely studied, though little has been reported about NTO and DNAN impact. Due to their novelty, little has been described about the toxicity and persistence of IHE chemicals in the environment, raising the question about how to assess their environmental impact.

Table 1. Physico-chemical properties of an IHE formulation, compiled from a [10], b [11] and c [12]

IHE formulation	Molecular structure	Percentage in formulation $(\%)_w$	Molecular weight (mg mol^{-1})	Solubility (20 °C) (mg L^{-1})
NTO $C_2H_2N_4O_3$	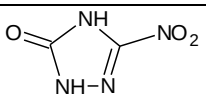	53	130.6	12800 a
DNAN $C_7H_6N_2O_5$	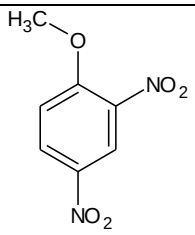	32	198.1	276 b
RDX $C_3H_6N_6O_6$	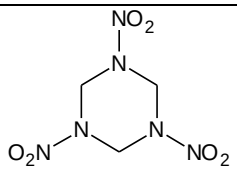	15	222.1	60 c

Once explosive residues are released into the environment, they may dissolve during precipitation and enter into the soil matrix. This process is called dissolution and it is the first step for studying explosive fate and transport in the environment [13]. Solubility is a thermodynamic process that measures the capacity of a solute to dissolve in a pure solvent. This describes the mass of solute that can be dissolved under specific conditions, but it cannot determine when or how fast it may happen. Conversely, dissolution rate is a kinetic process that defines the speed of a solute dissolution. For example, a solute may have low water solubility but it may dissolve fast or it may have a high solubility but take days to dissolve.

Dissolution rate is defined by the Noyes-Whitney equation [14]:

$$\frac{dm}{dt} = A * \frac{D}{d} * (C_s - C_b)$$

where dm/dt is the dissolution rate (kg s^{-1}); A is the contact area (m^2), D is the diffusion coefficient which is related to the viscosity of the solvent (m s^{-1}), d is the thickness of the concentration gradient (m); C_s is the solute surface maximum concentration (solubility) (kg L^{-1}) and C_b is the concentration of solute in the bulk solvent solution (kg L^{-1}).

During static conditions of no water movement, C_b approaches C_s, and there is no dissolution. Thus, it can be assumed that dissolution occurs only when water is moving past the particle as when it is raining, which is the case with the drop-impingent model. This approach is based on the drop-impingement dissolution model, which consists of the addition of individual rain drops impinging on small particles and it can be described as [15,16]:

$$\frac{dm}{dt} = -q * A_c * C_s$$

where q is the rainfall rate (L m^{-2} s^{-1}), A is the contact area (m^2) and Cs is the concentration of solute in the solvent (kg L^{-1}).

However, the use of dripping tests performed in the laboratory can be time consuming and expensive, due to the cost associated to material and equipment. To overcome this limitation, the use of computational programs for studying environmental fate and transport of pollutants in the environment is increasing due to the economical and time-saving advantages they offer against the traditional laboratory or field methods [17]. They enable the simulation of evolving systems based upon a simplified set of assumptions, and established conditions. However, they require data specific to the system that must be obtained either by literature review or experimentally. This issue is therefore a particular challenge for modelling the fate and transport of explosive residues as a) there is a lack of empirical data for the key parameters in the simulations and b) not many computational models have been used for studying explosive fate and transport.

GoldSim is a one-dimensional probabilistic computational program able to simulate the fate and transport of contaminants in different environments. It can simulate complex systems whose behaviour is either poorly understood or difficult to predict such that they have a high degree of uncertainty. Although it has not been extensively used for studying explosive transport in the environment, it has been successful for other organic compounds such as aromatic hydrocarbons [18] which share structural similarities with IHE constituents such as DNAN. Further to this, GoldSim enables the study of both discrete and continuous processes, which is important for contaminant dissolution in which, for instance the excess or lack of rain influences solubilisation. Finally, GoldSim has a Contaminant Transport Module, which has been successfully used for several environmental risk assessment purposes and pollutant types [19,20]. This last feature makes GoldSim interesting and useful for this study.

Therefore, the aim of this study was to develop a simple but representative computational model to simulate the rate of dissolution of DNAN, NTO and RDX from an IHE formulation using GoldSim. This was achieved by a) conducting visual and analytical laboratory experiments to understand the evolving external structure of the IHE, b) determining individual dissolution rates of the IHE compounds and c) using experimental data as inputs for the model in GoldSim. This initial study will serve as the basis to estimate the persistence of IHE compounds in the environment under more complex scenarios. This study will shed some light on how IHE formulations behave and will establish the bases for risk assessment purposes and environmental remediation strategies.

2. Material and methods

2.1 IHE formulation flakes and solvents

NTO (Chemring Nobel AS 2013) was manufactured in-house following a patented synthesis method [21]. DNAN (Sigma-Aldrich 2012) was purchased from Alfa Aesar (Thermo_Fisher 2018), both RDX (Gjersøe 2011) and an IHE formulation containing DNAN, NTO and RDX was already available at Cranfield University.

Acetonitrile was purchased from Sigma-Aldrich and ultra-pure water was obtained from Merck-Millipore.

2.2 Physical measures.

Three IHE flakes between 30 and 60 mg were chosen to study their dissolution under specific conditions. The flakes were selected to simulate representative small residues from an open burning detonation. Although in reality there would likely be more than one flake in an area, the experiment focused on the study of an average flakes mass. The IHE flakes weighed before the experiments with the aim to control and quantify the mass dissolved. The length, width and height were measured and any physical irregularity in the flake was written down. In addition, pictures of the flakes were taken with a digital camera (Samsung NX 300) before and after the dripping test to compare the IHE structure and to observe any visual change during the experiment.

2.3 Dissolution ‘drip’ tests of the IHE formulation

Three flakes of the IHE were placed in Pyrex Buchner funnels, held by a support stand and clamps. The flakes were exposed to a continuous flow of water at 40 mL min^{-1} (Kramoer Dosing Pump, China) for 100 minutes, with a total volume of 4L of distilled water to simulate

rainfall. The water flow was directed onto the flakes using a framework to keep the influent tube steady. The distilled water had an initial pH=6.2 ± 0.1 and was stored at room temperature (20 ± 1 C). Leachate was collected every 5 minutes during the first 50 minutes and every 10 minutes over another 50 minutes using 300 mL amber glass jars placed under the funnels (**Figure 1**). 2 mL aliquots were filtered through a 0.2 µm polyethylene terephthalate (PET) filters and stored at 4 °C, until analysis (within 2 days).

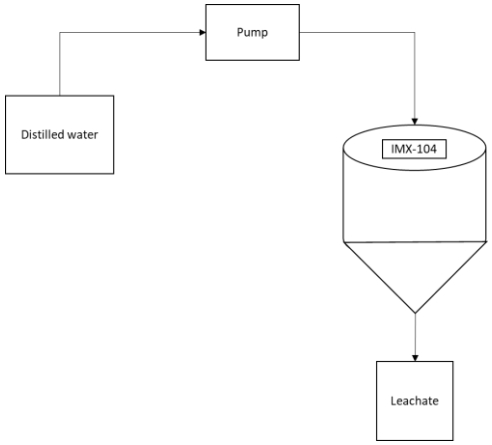

Figure 1. Schematic illustration of the experimental setup for the study of the IHE formulation dissolution rate

2.4 High Performance Liquid Chromatography with Diode Array Detector (HPLC-DAD)

HPLC was performed using a Waters-Alliance 2696 equipped with a Waters 996 photodiode array detector (USA). The analytes were separated on a ZORBAX Eclipse Plus C18 column (4.6 x 150 mm, i.d. 3.5 µm) from Agilent Technologies (Wilmington, DE, USA) maintained at 30°C. Samples were injected with a syringe loading injector fitted with 10 µL loop. Optimum chromatographic conditions were obtained with a linear gradient of 40% ACN (solvent A) and 60% water acidified 0.1% with formic acid (solvent B) with a flow rate of 1.5 mL min^{-1}. The analytes were quantified via UV absorbance with optimum sensitivity detected at 296 nm for DNAN, 245 nm for RDX and 315 nm for NTO. Retention times were 1.01 minutes for NTO, 3.15 minutes for RDX and 4.96 minutes for DNAN. The calibration curve was obtained by plotting the concentration against corresponding peak area for each analyte and both peak areas of samples and standards were determined by Empower 2 software (Waters). For this method, the limit of quantification was between 0.40 and 0.45 mg L^{-1} and the limit of detection was 0.04-0.05 mg L^{-1} for NTO, DNAN and RDX [1].

2.5 GoldSim simulation

GoldSim version 12.1 and the Contaminant Transport Module were used with the Material, Pathway, Selector, Functions as well as Result elements [22]. The properties of the water and explosive compounds were defined in the element 'Material' which includes molecular mass and solubility. The Pathway elements included a Pipe element (frit funnel) where the dimensions were specified and it was connected to a Sink element (leachate) (**Figure 2**).

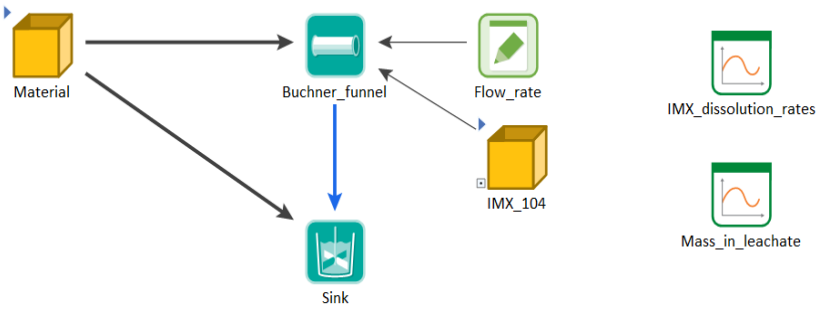

Figure 2. GoldSim scheme for the dissolution rate of the IHE formulation

Parameters such as initial mass, percentage of explosive chemicals in the formulation and water flow rate were also included in the model as 'Data' elements and linked between them by 'Expression' elements. Individual dissolution rates were added as a 'Stochastic' element with their respective standard deviation and linked to the system with a 'Selector' element that allowed the definition of the specific dissolution rate for each compound over time. Finally, a 'Result' element was defined to show the cumulative individual mass in the leachate.

Simulations were run with a stochastic approach, using the Monte Carlo method available in the computational program and performing 101 realizations. The simulations were run over 100 minutes, to simulate the dripping tests and data was reported every 5 minutes.

3. Results and discussion

3.1 Comparison of the flakes before and after the experiment by digital camera

Photographs of three IHE flakes were taken at the beginning and partway through the dissolution tests after 100 minutes (**Figure 3**). Initially, the flakes were yellow in colour, most likely from the NTO content (53%) in the formulation. Overall, the flakes had a flat structure due mainly to the way the flakes are formulated.

After dripping water (2L) onto the flake for 50 min, small pores were observed on the surface of the flake. In addition, the flake becomes paler, and the collected leachate was observed to have a slightly yellow tinge. This is mainly due to dissolved NTO, which has the highest

proportion in the flake (53%) and is significantly more soluble in water than RDX and DNAN [23]. Finally, after dripping water for 100 min (4L) the flakes lost their colour and more small pores were observed. The flakes became more brittle and easier to break due to the lack of consistency in their structure. Visually, the flakes were slightly smaller in comparison to the initial ones, although it was not noticeable in all cases.

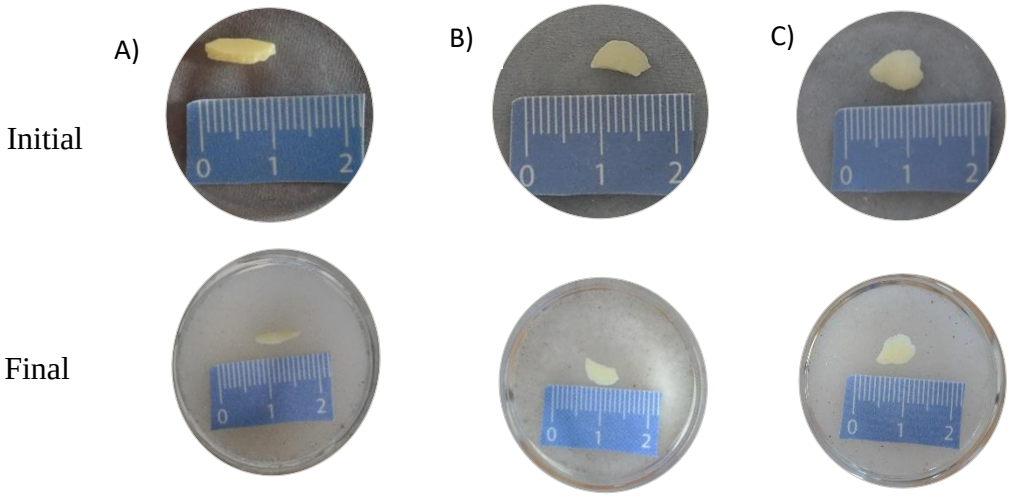

Figure 3. Digital photograph of IHE flakes before and after the dripping tests (4L) showing the discolouration and mass loss.

3.2 Dissolution rate of NTO, DNAN and RDX

Laboratory drip experiments were conducted to measure the dissolved mass of each constituent in the IHE formulation as a function of water volume for three replicates. The mass balance shows the total mass of dissolved and remaining IHE (Table 3)

Table 3. Mass balance of IHE flakes by HPLC and gravimetric methods.

Flake	Mass (mg) scale			Mass (mg) HPLC	Relative Difference (%)
	Initial	Final	Dissolved	Dissolved	
A	57.5	37.7	19.8	20.4	2.9
B	34.3	26.0	8.3	10.9	23.6
C	64.4	46.4	18.0	19.8	9.0

The initial mass of the flakes varied between 34.4 to 64.4 mg, which was chosen randomly to representatively calculate an average of the dissolved mass and dissolution rates. A lower quantity of dissolved mass was found in flake B mainly due to the lower initial mass (60% and 53% respectively) in comparison to flakes A and C. However, a higher dissolved mass was found in flake A than in flake C despite the initial mass of flake C being 10% higher. Therefore, there is a direct relationship between the initial mass and the mass dissolved, although when the initial masses are similar the relation can slightly vary.

The comparison between the dissolved mass calculated by HPLC and by gravimetric methods (scale) at the end of the experiment allows the verification of the results obtained by HPLC. In all of the cases, the mass determined by HPLC was higher, being 23% for flake B and only 2.9 and 9.0% for flakes A and C respectively. This can be explained by systematic errors in the equipment and due to the addition of small masses obtained by HPLC against a single measure for gravimetric methods.

The average of the individual percentage of the chemical compounds in the flakes was plotted in a bar graph (**Figure 4**). NTO shows a higher dissolution percentage (37.3%) whereas DNAN and RDX only had 25.5% and 26.2% of their masses dissolved respectively. Therefore, once the IHE formulation starts to dissolve, the ratio of the compounds in the flake changes as NTO tends to dissolve faster. This fact was can be supported by the visual observations, with the conclusion that the observed pores were mainly due to NTO dissolution from the DNAN matrix [23]. Regarding DNAN and RDX, the percentage dissolved is similar, showing that despite the differences in the initial individual mass in the flake, the ratio of these chemical compounds in the flake is similar.

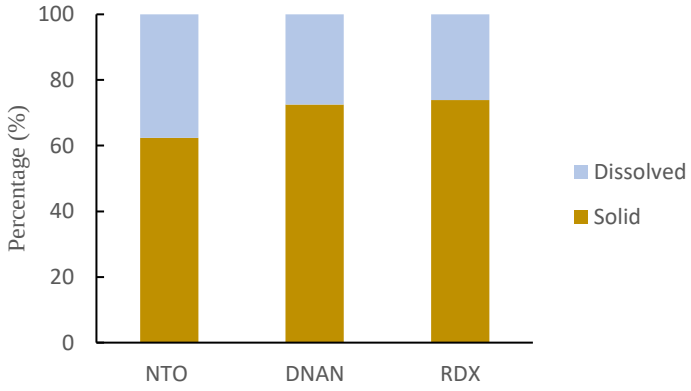

Figure 4. Percentage of NTO, DNAN and RDX (average) dissolved (blue) and remaining (khaki) in the flake after the dripping tests.

The percentage of cumulative mass dissolved for each constituent in the IHE formulation was plotted against time (**Figure 5**). The percentage cumulative mass was calculated by adding the mass of each constituent measured in the water samples over time. The plots highlight compositional variations among the flakes and indicate how they behave in relation to their initial mass.

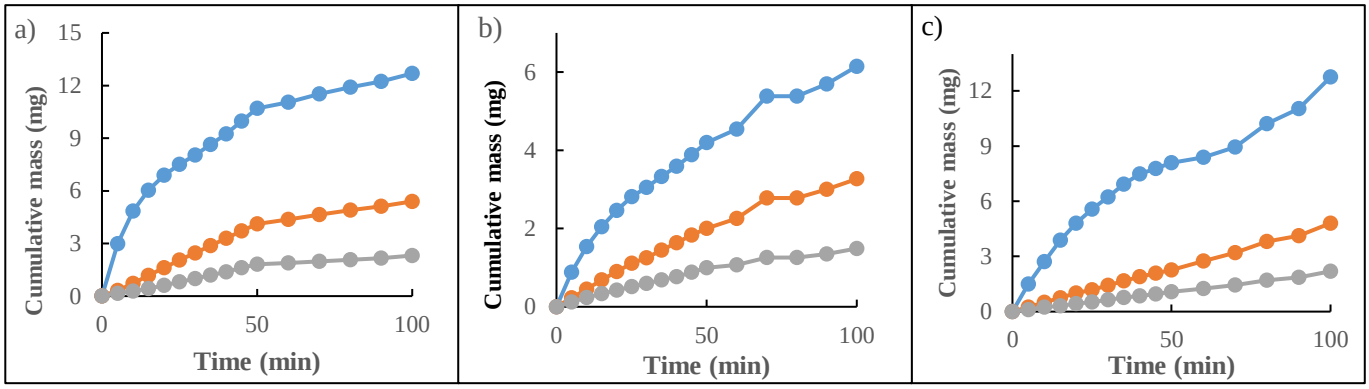

Figure 5. Dissolved cumulative mass of the IHE compounds over time of flake A (a), flake B (b) and flake C (c). The lines show NTO (blue), DNAN (orange) and RDX (grey).

As expected, based on solubility, NTO dissolves first, followed by DNAN and finally RDX. The dissolution rate of NTO is higher at the start of the test and decreases during the test. This is due to the decreasing mass of NTO available for dissolution in the flake, and the increasing need for water to penetrate the DNAN matrix to dissolve exposed NTO[11,24].

Experimental individual dissolution rates were obtained by calculating the slope of the cumulative mass over time (**Table 4**). For NTO, three different slopes were identified going from 0 to 15 minutes, from 15 to 50 minutes and from 50 until the end of the dripping test. For DNAN and RDX, only two different sections were distinguished, from 0 to 50 minutes and from 50 to 100 minutes.

Table 4. Average and standard deviation (S.D.) of individual dissolution rates (mg min^{-1}) of the IHE chemical compounds over time

	Dissolution rate (mg min^{-1})					
	NTO		DNAN		RDX	
Time	Average	S.D.	Average	S.D.	Average	S.D.
0-15 min	0.264	0.107	0.056	0.020	0.026	0.008
15-50 min	0.105	0.029				
50-100 min	0.057	0.026	0.033	0.012	0.014	0.006

Individual dissolution rates inform when the compounds in the flake are dissolved and how much. Generally, the rates decrease over time as flake shrinks and the surface area is lower. NTO has the highest dissolution rate mainly due to its high solubility in water and its significant mass within the IHE formulation. After 15 minutes, the dissolution rate halved and after 50, it decreased four times compared to the initial one. Conversely, DNAN dissolution rate only decreases 40%, and RDX dissolution rate 53%.

Nevertheless, this dripping test only informs of the behaviour of the compounds in the initial dissolution stage. It would be necessary to continue the dripping test to observe whether these dissolution rates are constant over time or by contrast, they continue decreasing. To overcome this limitation, simulations in GoldSim can help to avoid long-time and expensive laboratory experiments. Nonetheless, to rely on the simulations and make them representative enough, they need some experimental inputs and previous validation.

3.3 Simulation in GoldSim

An initial simulation validating the model developed in GoldSim to study the dissolution rates of the IHE formulation. Their dependency on the mass has been tested using the average dissolution rates with their standard deviation and the Monte Carlo method. To represent and validate the model, it has been compared with flake C, chosen randomly among the three flakes. The cumulative percentage mass dissolved has been plotted against time, being the percentage of mass dissolved the ratio between the mass dissolved divided by the initial mass of the flake (**Figure 6**).

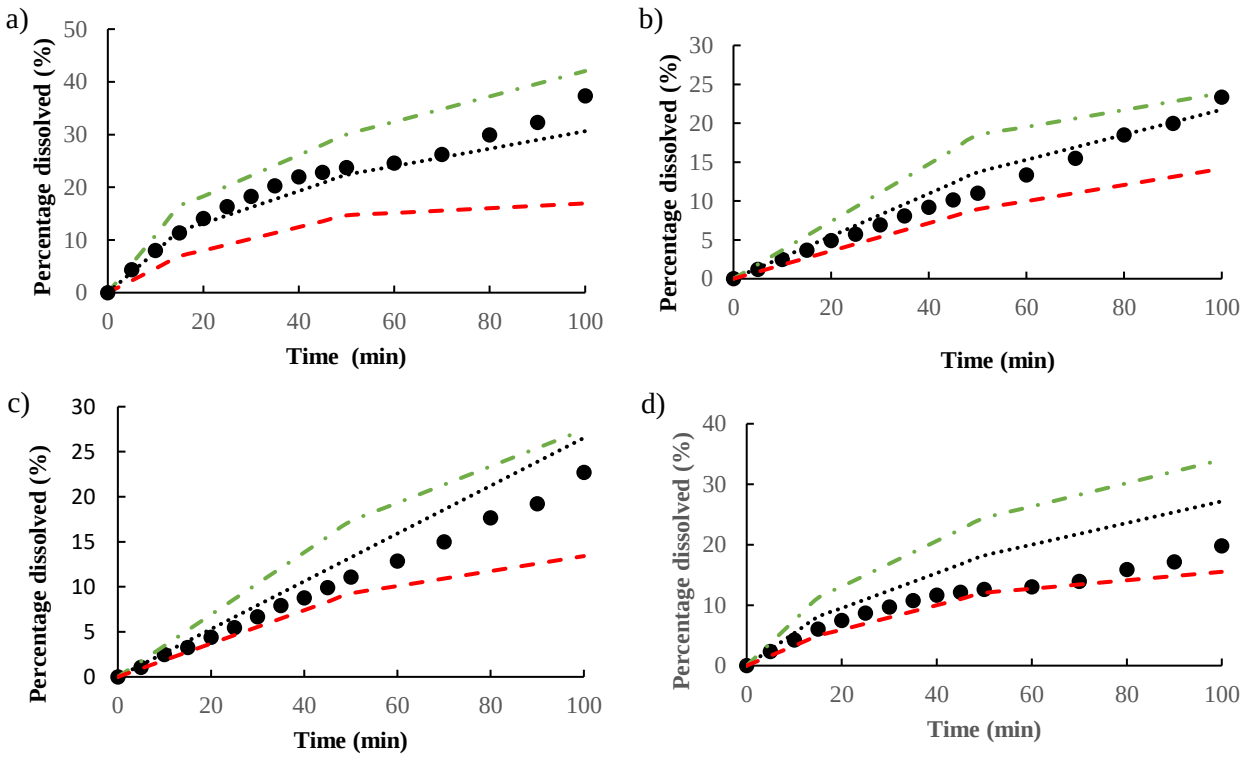

Figure 6. Comparison between the GoldSim simulation, including dissolution rates as a distribution element and 101 realizations using Monte Carlo, and laboratory experiment dissolution rate curves for NTO (a) DNAN (b) RDX (c) and the IHE (d). The dots indicate experimental results and the discontinuous line is the simulated results from GoldSim. Green, red and black discontinuous lines indicate maximum, minimum and mean breakthrough, respectively.

In all cases, experimental results are inside of the maximum and minimum dissolution rates, although this was expected as experimental data of flake C was used to calculate dissolution rates. Therefore, the model cannot be validated this way, although it is guidance to address any issues and mistakes in the model. One way to validate the model would be by performing experimental dripping tests on new flakes of the same size and mass and compare results with the model. However, as mentioned before, flake C has been used here as an example.

Though similar, the dissolved NTO is higher in percentage than in DNAN and RDX for both simulated and experimental curves. After 100 minutes, simulated cumulative mass for NTO varied between 42% (maximum) and 17% (minimum), showing high differences due to the high standard deviation obtained experimentally. For DNAN, between 14% (minimum) and 24% (maximum) was dissolved after 100 minutes. Regarding RDX, the cumulative dissolved mass reached was similar, but with a broader range, going from 13% to 27% of the RDX initial mass.

Finally, an estimated dissolution time for the entire flake was simulated in GoldSim by supposing constant dissolution rate from 50 minutes onwards. This approximation might not be representative enough of a real dissolution process in the environment, but it gives an estimated time of when the flakes are expected to completely dissolve and therefore pass into the soil or water in the environment (**Table 5**). Then, an estimation of a potential real environment was made using the average rainfall in Wiltshire, UK obtained from the Weather station in Marlborough (UK) and the water dropped to the flakes per area (Pyrex Buchner funnel).

Table 5. Prediction of when the explosive flake dissolves entirely.

	NTO		DNAN		RDX	
	GoldSim (minutes)	Estimation (months)	GoldSim (minutes)	Estimation (months)	GoldSim (minutes)	Estimation (months)
Flake A	403	12	469	14	531	16
Flake B	186	6	246	7	279	8
Flake C	468	14	535	16	606	18

In the three cases, time predicted to dissolve NTO is faster than for DNAN and RDX, being between 6 and 14 months in real time. DNAN dissolution rate is slightly slower, dissolving between 7 and 16 months. Finally, RDX is the slowest to dissolve, needing between 8 to 16 months to fully dissolve. Thus, a flake between 30 and 60 mg would require up to 16 months to completely dissolve in Wiltshire, UK.

4. Conclusions

With the drive for insensitive munitions, it is likely that IHE filled munitions will increasingly be used for training and defence purposes. Therefore, understanding the behaviour of these IHE prior to their extensive use is essential. Dissolution rates are key in the movement of IHE through the soil as they determine when and how much these chemicals pass through the soil solution.

The visual comparison of the flake appearance along with the dripping tests provide us with information necessary to understand how these chemicals behave in combination. The visual pictures show a fast dissolution of NTO in the flake that leaves pores and decolours the flake from an intense yellow to barely white. It could be interesting to observe the structure under a microscope to complete the information and compare the evolution of the surface area to the initial one.

The dripping tests show how the dissolution process of the IHE compounds over time. NTO dissolved remarkably faster than DNAN and RDX despite its presence in the flake being higher. Dissolution rates were very different for the same compounds and not constant over time, which hampered its determination and potential use to assess environmental impact caused by IHE residues.

The model developed in GoldSim was simple but enabled the potential understanding of how the explosive compounds behave when they are in the environment. The use of the stochastic approximation has allowed the determination of the potential mass of the chemical that can be found in the soil once they are released. The model still needs to be validated but it has served as a basis for further simulations. In addition, initial estimations of the required time necessary to dissolve in Wiltshire were key in assessing when and how much these chemical compounds enter into the environment system.

The next stage will be to continue increasing the complexity of the system by testing larger systems, using rain water to be gain representativeness and testing different exposure scenarios e.g. lower temperatures or acid water. The ultimate stage of the project is to create a representative model able to simulate the fate and transport of explosives in the environment able to assess environmental risks and help remediation strategies caused by IHE.

References

1. Temple T., Ladyman M., Mai N., Galante E., Ricamora M., Shirazi R., et al. Investigation into the environmental fate of the combined Insensitive High Explosive constituents 2,4-dinitroanisole (DNAN), 1-nitroguanidine (NQ) and nitrotriazolone (NTO) in soil. Science of the Total Environment. 2018; 625: 1264–1271. Available at: DOI:10.1016/j.scitotenv.2017.12.264

2. Chappell MA., Seiter JM., West HM., Miller LF., Negrete ME., Lemonte JJ., et al. Geoderma Predicting 2 , 4-dintroanisole (DNAN) sorption on various soil " types " using different compositional datasets. Geoderma. Elsevier; 2019; 356(August): 113916. Available at: DOI:10.1016/j.geoderma.2019.113916

3. Inglezakis VJ., Zorpas A. Industrial hazardous waste in the framework of EU and international legislation. Management of Environmental Quality: An International Journal. 2011; 22(5): 566–580. Available at: DOI:10.1108/14777831111159707

4. Vila M., Lorber-Pascal S., Laurent F. Phytotoxicity to and uptake of TNT by rice. Environmental Geochemistry and Health. 2008; 30(2): 199–203. Available at: DOI:10.1007/s10653-008-9145-1

5. Lotufo GR., Biedenbach JM., Sims JG., Chappell P., Stanley JK., Gust KA. Bioaccumulation kinetics of the conventional energetics TNT and RDX relative to insensitive munitions constituents DNAN and NTO in Rana pipiens tadpoles. Environmental Toxicology and Chemistry. 2015; 34(4): 880–886. Available at: DOI:10.1002/etc.2863

6. Madeira CL., Field JA., Simonich MT., Tanguay RL., Chorover J., Sierra-Alvarez R. Ecotoxicity of the insensitive munitions compound 3-nitro-1,2,4-triazol-5-one (NTO) and its reduced metabolite 3-amino-1,2,4-triazol-5-one (ATO). Journal of Hazardous Materials. Elsevier B.V.; 2018; 343: 340–346. Available at: DOI:10.1016/j.jhazmat.2017.09.052

7. Zhao J-S., Monteil-Rivera F., Thiboutot S., Groom C., Hawari J., Halasz A., et al. Fate and Transport of Explosives in the Environment. Ecotoxicology of Explosives. 2009; : 5–33. Available at: DOI:doi:10.1201/9781420004342.ch2

8. Temple TJ., Ladyman MK. Scientific principles of environmental management. Global Approaches to Environmental Management on Military Training Ranges. 2019. 1–25 p. Available at: DOI:10.1088/978-0-7503-1605-7ch1

9. Pichtel J. Distribution and fate of military explosives and propellants in soil: A review. Applied and Environmental Soil Science. 2012; 2012: 1–33. Available at: DOI:10.1155/2012/617236

10. Spear RJ., Louey CN., Wolfson MG. A preliminary assessment of NTO as an insensitive high eplosive. MRL technical report MRL-TR-89-18. 1989;

11. Taylor S., Ringelberg DB., Dontsova K., Daghlian CP., Walsh ME., Walsh MR. Insights into the dissolution and the three-dimensional structure of insensitive munitions formulations. Chemosphere. 2013; 93: 1782–1788. Available at: DOI:10.1016/j.chemosphere.2013.06.011

12. Pennington JC., Brannon JM. Environmental fate of explosives. Thermochimica Acta. 2002; 384: 163–172. Available at: DOI:10.1016/S0040-6031(01)00801-2

13. Dortch MS. Modeling Dissolution of High Explosive Formulations. Soil and Sediment Contamination. 2018; 27(4): 280–310. Available at: DOI:10.1080/15320383.2018.1472209

14. Byrn SR., Zografi G., Chen XS. Solubility and Dissolution. Solid State Properties of Pharmaceutical Materials. 2017; : 249–264. Available at: DOI:10.1002/9781119264408.ch17

15. Taylor S., Lever JH., Fadden J., Perron N., Packer B. Simulated rainfall-driven dissolution of TNT, Tritonal, Comp B and Octol particles. Chemosphere. Elsevier Ltd; 2009; 75(8): 1074–1081. Available at: DOI:10.1016/j.chemosphere.2009.01.031

16. Lever JH., Taylor S., Perovich L., Bjella K., Packer B. Dissolution of composition B detonation residuals. Environmental Science and Technology. 2005; 39(22): 8803–8811. Available at: DOI:10.1021/es050511r

17. Whelan M., Ramos AM., Villa R., Guymer I., Jefferson B., Rayner M. Environmental science. Environmental Science: Processes and Impacts. 2018; 20: 737–856. Available at: DOI:10.31729/jnma.1240

18. Cao X., Temple T., Li X., Coulon F., Sui H. Influence of particle size and organic carbon content on distribution and fate of aliphatic and aromatic hydrocarbon fractions in chalks. Environmental Technology and Innovation. 2015; 4: 227–239. Available at: DOI:10.1016/j.eti.2015.09.001

19. Bhuyian NM., Thornton J., Kalyanapu A. Developing “Flood Loss Curve” for City of Sacramento. 2015 ASFPM Conference. 2015; : 1–8. Available at: https://www.asfpmfoundation.org/ace-images/Developing_Flood_Loss_Curve_for_City_of_Sacramento.pdf

20. Havlová V., Vopálka D. HTO as a conservative tracer used for characterization of contaminant migration in porous rock environment. Journal of Radioanalytical and Nuclear Chemistry. December 2010; 286(3): 785–791. Available at: DOI:10.1007/s10967-010-0723-1

21. Lee K., Coburn M. 9165: 3-Nitro-1,2,4-triazol-5-one, a less sensitive explosive. United States of America; 1988.

22. GoldSim Technology Group. GoldSim User’s Guide v12.1. 2018.

23. Taylor S., Park E., Bullion K., Dontsova K. Dissolution of three insensitive munitions formulations. Chemosphere. Elsevier Ltd; 2015; 119: 342–348. Available at: DOI:10.1016/j.chemosphere.2014.06.050

24. Richard T., Weidhaas J. Dissolution, sorption, and phytoremediation of IMX-101 explosive formulation constituents: 2,4-dinitroanisole (DNAN), 3-nitro-1,2,4-triazol-5-one (NTO), and nitroguanidine. Journal of Hazardous Materials. Elsevier B.V.; 2014; 280: 561–569. Available at: DOI:10.1016/j.jhazmat.2014.08.042